Interlayer coupling across semi-metallic iron monosilicide

B. Croonenborghs,[1] F.M. Almeida,[1] C. L'abbé,[1] R.R. Gareev,[2] M. Rots,[1] A. Vantomme,[1] and J. Meersschaut[1,*]

[1] *Instituut voor Kern- en Stralingsfysica, K.U.Leuven, Celestijnenlaan 200D, B-3001 Leuven, Belgium*
[2] *Institut für Festkörperforschung, Forschungszentrum Jülich GmbH, D-52425 Jülich, Germany*

(Dated: October 12, 2004)

We studied the interlayer exchange coupling between Fe films across iron monosilicide spacer layers with the metastable CsCl structure. The bilinear (J_1) and the biquadratic (J_2) coupling strengths are determined by fitting the in-plane easy- and hard-axis magnetization curves. Both coupling coefficients have a strong, non-monotonous temperature dependence and vary exponentially as a function of the spacer thickness. The temperature dependence of the coupling constants is explained within the framework of Slonczewski's loose spin model [J. Appl. Phys. **73**, 5957 (1993)] in which a decrease of the loose spin concentration upon cooling is introduced. The exponentially decaying coupling strength with increasing spacer layer thickness is attributed to the semi-metallic nature of the metastable monosilicide phase.

PACS numbers: 75.70.Cn, 75.50.Bb, 75.30.Et,73.61.At
Keywords: interlayer coupling,loose spin,CsCl-FeSi, semi-metal

I. INTRODUCTION

The idea of exploring interlayer coupling across non-metallic layers sparked off a big interest in the coupling of Fe films across Si-containing spacers[1–4]. Fe and Si have a strong tendency to form silicides[5] and different types of Fe-silicides may be stabilized, depending on the preparation methods and conditions used. This considerably complicates studies addressing the relation between silicide formation and interlayer coupling. In the present work we restrict ourselves to Fe-silicide spacers with the metastable CsCl structure.

The qualitative behavior of the exchange coupling across iron silicide with the CsCl structure is very sensitive to the exact spacer composition. Strong antiferromagnetic interlayer coupling, varying exponentially with the spacer layer thickness, was reported in Fe/Si/Fe structures grown with molecular beam epitaxy (MBE)[6]. The observed coupling is mediated by a non-stoichiometric silicon rich spacer with a metastable CsCl structure, formed by Fe diffusion into the Si spacer[7]. For a homogenous and iron rich MBE-grown CsCl-$Fe_{0.56}Si_{0.44}$ spacer, on the other hand, an oscillatory interlayer coupling as a function of spacer thickness was found[8].

In this paper, we present a detailed study of the interlayer coupling across homogenous, stoichiometric CsCl-$Fe_{0.50}Si_{0.50}$ spacer layers grown with MBE. The observed exponential thickness dependence of the coupling strength is ascribed to the semi-metallic nature of the metastable monosilicide phase.

Apart from bilinear exchange coupling, also a strong biquadratic contribution to the coupling has been observed in sputtered Fe/Si multilayers[9–12]. In Fe/Si-based superlattices a detailed investigation of the biquadratic coupling was impossible due to vertical variations of the coupling properties[12]. Also in sandwich structures the origin of the biquadratic coupling mechanism is still a matter of debate. Strijkers *et al.*[6] favored the loose spin model[13] to interpret the biquadratic contribution to the coupling in Fe/Si/Fe structures, while Gareev *et al.*[8] discussed the temperature dependence of the biquadratic coupling in Fe/CsCl-$Fe_{0.56}Si_{0.44}$/Fe in terms of thickness or composition fluctuations[14].

Here, we find strong evidence, based on combined measurements of the temperature and the thickness dependence of the bilinear (J_1) and the biquadratic (J_2) coupling constants, that paramagnetic entities acting as loose spins mediate the biquadratic exchange across monosilicide spacer layers. The loose spins are also found to contribute substantially to the bilinear coupling.

II. EXPERIMENTAL DETAILS

Epitaxial Fe(80 Å)/FeSi/Fe(40 Å) sandwiches are grown with molecular beam epitaxy on polished MgO(001) substrates held at 150°C. The pressure during growth was below 4×10^{-10} Torr. The iron constituting the ferromagnetic films has the natural isotopic composition whereas for the silicide layers Si is codeposited with isotopically enriched ^{57}Fe (95%). We used calibrated quartz crystal monitors to control the thickness, the deposition rate and the relative atomic flux. The deposition rates for ^{57}Fe and Si were 0.030 Å/s and 0.051 Å/s, respectively. The spacer thickness (t_{FeSi}) was varied from 8 to 30 Å. Finally, the samples were capped with 45 Å of Au, deposited at room temperature, to prevent oxidation. Well-defined RHEED patterns are maintained throughout the whole deposition sequence and indicate epitaxial growth.

Thanks to the selective ^{57}Fe enrichment in the spacer layer, conversion electron Mössbauer spectroscopy (CEMS) measurements are mainly sensitive to the silicide layer. CEMS experiments, performed at room temperature, reveal the presence of a well-defined crystalline CsCl monosilicide in all samples[15]. Low angle X-ray reflectivity measurements exhibit clear oscillations up to

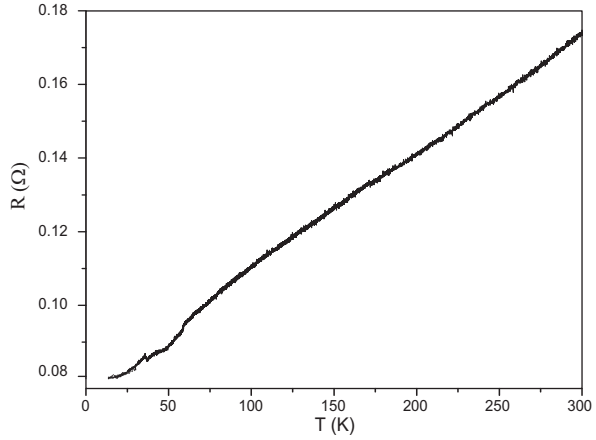

FIG. 1: Temperature dependent resistance in CPP geometry for a trilayer with t_{FeSi}=26 Å and a junction size of 9 μm^2.

$2\theta = 16°$, indicative of excellent layering with both low intermixing and low structural roughness.

The resistance R of the trilayers in current perpendicular to plane (CPP) geometry gives information about the electronic nature of the monosilicide phase. Resistance measurements are performed as in ref. 16 for various junction sizes on a trilayer with t_{FeSi}=26 Å, grown on a 1500-Å-thick Au(001) buffer. We verified that the presence of the Au buffer does not affect the spacer layer properties by comparing the CEMS spectra and the hysteresis curves for the trilayers with and without a Au buffer. Figure 1 shows the temperature dependent resistance for a junction size of 9 μm^2. At room temperature we find R $\approx$ 0.175 Ω, which corresponds to a resistivity $\rho \approx 6.1 \times 10^4$ $\mu\Omega$cm. This is several orders of magnitude bigger than for pure iron, but it is still markedly less than for semiconducting or isolating materials[16]. This, in combination with the observation of linear I-V curves and a positive temperature coefficient for the resistance, indicates a semi-metallic nature of monosilicide interlayers with the CsCl structure.

Finally, the magnetic properties of the samples are investigated by means of hysteresis loops, taken between 10 K and room temperature with a vibrating sample magnetometer (VSM).

III. ANALYSIS OF THE MAGNETIZATION CURVES

In figure 2, normalized easy-axis hysteresis loops measured at 290 K and at 20 K are shown for samples with spacer thickness t_{FeSi} = 14 Å and t_{FeSi} = 16 Å. Going from high to low fields three well-defined states can be identified: the parallel, the orthogonal and the antiparallel alignment of the magnetic moments in the two iron layers. While the magnetization of the 80-Å-thick bottom Fe layer is always effectively pinned by the magnetic field, the moment in the thinner top Fe layer (40 Å) rotates and eventually reverses its direction. This way, at room temperature a remanence (M_R/M_S) of 0.33 is obtained, corresponding to perfect antiparallel alignment of both magnetic moments at zero field.

We have determined the cubic anisotropy constant (K_c), assumed equal for both iron layers, and the bilinear (J_1) and the biquadratic (J_2) exchange coupling constants as a function of monosilicide thickness and temperature from simultaneous fits of the easy- and hard-axis hysteresis loops. The magnetization is calculated for each applied field by minimizing the phenomenological areal free energy expression including Zeeman, cubic anisotropy and exchange coupling terms. Here, the interlayer exchange coupling is described as

$$E_{ex} = -J_1\cos(\theta) - J_2\cos^2(\theta), \qquad (1)$$

where θ is the angle between the magnetization of both Fe films. J_1 represents the bilinear coupling which aligns the magnetic moments parallel ($J_1 > 0$) or antiparallel ($J_1 < 0$). J_2 describes the biquadratic coupling which favors a perpendicular alignment of the magnetizations for $J_2 < 0$. We were able to separate the bilinear and

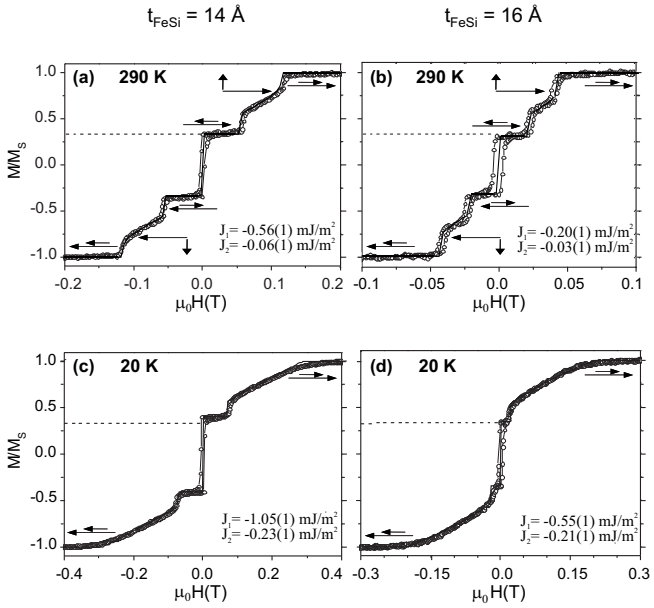

FIG. 2: Magnetization curves for Fe(80 Å)/$^{57}Fe_{0.50}Si_{0.50}$/Fe(40 Å) trilayers measured with the magnetic field applied along an in-plane easy axis. The solid lines are the fitted curves using the model described in the text. The deduced values for the coupling parameters are given in the different panels. The arrows indicate the direction of the magnetization in the bottom Fe layer (long arrow) and the top Fe layer (small arrow). The dashed lines give the remanent magnetization in case of perfect antiparallel alignment of the magnetic moments in the two iron layers. Note the different magnetic field ranges used for the various panels.

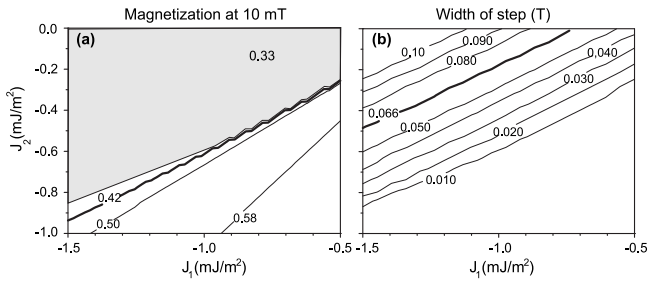

FIG. 3: Theoretical contour plots of the magnetization at 10 mT (a) and the width of the step near remanence (b) for a wide range of coupling strengths in expression 1. The shaded area in panel (a) represents the region with a remanence of 0.33.

the biquadratic coupling coefficients for all samples, except for the thinnest sample (t_{FeSi} = 8 Å), where the loops exhibit a convex shape rather than the presence of plateaus. For all samples, we found a value for the cubic anisotropy constant close to that for bulk, indicating good epitaxial quality of both iron layers.

Figure 2 shows that an increase in remanence develops upon cooling. A value of approximately 0.42 is reached at 20 K for a sample with t_{FeSi}=14 Å. We calculated the magnetization near remanence (at 10 mT) as a function of the coupling strengths J_1 and J_2 based on expression 1. The result is plotted in fig. 3(a), where the shaded area represents the area with a magnetization that reflects an antiparallel alignment of the magnetic moments of both iron films. The thick solid line indicates the desired magnetization of 0.42. We also calculated the width of the step that appears near remanence in the magnetization curve as a function of J_1 and J_2. The results are presented in figure 3(b). Here, the solid line indicates a width of 66 mT, as is observed in the magnetization curve in fig. 2(c). No crossover with the solid line of panel 3(a) is found. This excludes an interpretation of the rise in remanent magnetization in terms of expression 1 only. We therefore added a contribution with a square hysteresis loop to a dominating antiferromagnetic behavior. The weight of the latter is labelled the antiferromagnetically coupled fraction (F). When a step is present in the magnetization curve, F can be determined directly from the experimental measurements as

$$F = 1.5 \times [1 - \frac{M_R}{M_S}]. \quad (2)$$

This analysis permits one to correctly describe the steps in the magnetization curve of fig. 2(c) with F=0.88(1), J_1= -1.05(1) mJ/m^2 and J_2=-0.23(1) mJ/m^2. More general, the model allows to satisfactorily fit the hysteresis curves at various temperatures for the different samples (e.g. solid lines in fig. 2).

IV. TEMPERATURE DEPENDENCE OF THE INTERLAYER COUPLING

Figure 4 shows the saturation field (defined as the value of the applied magnetic field where the magnetization reaches 90% of its saturation value), the remanent magnetization, the coupling constants, J_1 and J_2, and the antiferromagnetically coupled fraction as a function of temperature for a sample with t_{FeSi} = 14 Å. Both the biquadratic and the bilinear coupling coefficient increase strongly with decreasing temperature down to approximately 100 K, and then slightly decrease again. The same trend is observed in the measured saturation field (fig. 4(a)). Figure 4(d) reveals that the antiferromagnetically coupled fraction F decreases at temperatures below 100 K. These results suggest: (i) the same underlying mechanism for J_1 and J_2 and (ii) a relation between the antiferromagnetically coupled fraction and both coupling coefficients.

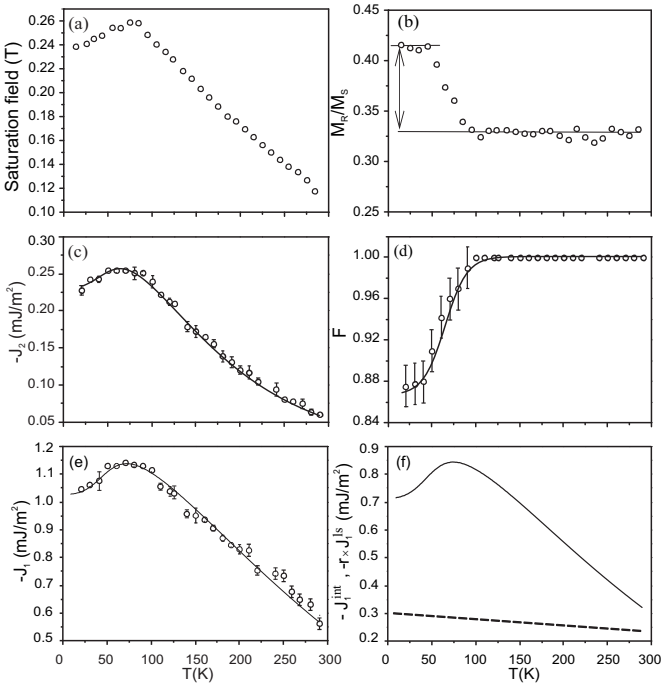

FIG. 4: Temperature dependence of the saturation field (a), the remanent magnetization (b), the exchange coupling parameters J_2 (c), F (d), J_1 (e) and J_1^{int} and r×J_1^{ls} (f) for a sample with t_{FeSi} = 14 Å. The solid lines in panels (c) and (e) are best fits obtained using the model described in the text. In panel (d) a Fermi-Dirac like function is used to model the antiferromagnetically coupled fraction F of the sample. The dashed line in panel (f) is the contribution of the intrinsic bilinear exchange J_1^{int}, whereas the solid line represents the reduced bilinear loose spin contribution r×J_1^{ls}.

A mechanism that can account for the observed magnitude and the strong temperature dependence of the biquadratic coupling in figure 4(c) is the loose spin model[13]. The model postulates that biquadratic coupling can be

mediated by paramagnetic entities present inside the spacer layer or adjacent to its interfaces. These so-called "loose spins" couple to both ferromagnetic layers via the indirect exchange potentials U_1 and U_2, respectively, leading to an additional contribution to the interlayer coupling. For a complete description of the model we refer to ref. 13. Because the loose spin model as introduced by Slonczewski cannot account for a non-monotonous temperature dependence of J_2, a temperature dependent loose spin concentration was previously introduced to describe this kind of behavior in certain Fe/Cr multilayers[17]. Here, we assume that the loose spins are laterally inhomogeneously distributed over the sample and that their fractional concentration has the same temperature dependence as the antiferromagnetically coupled fraction F. This implies that the fractional concentration of loose spins for a sample with t_{FeSi}=14 Å is constant on cooling down to approximately 100 K (Fig. 4(d)). In the temperature range below 100 K, however, the remanence rises because part of the paramagnetic entities become ineffective in mediating the biquadratic coupling between the ferromagnetic layers. This occurs in the regions of the sample that had the biggest local concentration of loose spins at room temperature. Therefore, below 100 K, the fractional loose spin concentration decreases. Noting that the loose spin contribution to the biquadratic interlayer coupling depends linearly on the fractional concentration of loose spins[13], this explains the observed reduction in J_2 below 100 K (Fig. 4(c)). Assuming an atomic spin S=1, the biquadratic coupling strength as a function of temperature is fitted with the interaction potentials U_1 and U_2 and the room temperature fractional concentration of loose spins c(RT) as free fitting parameters in Slonczewski's theory[13]. The resulting fit is displayed as the solid line in figure 4(c) and yields c(RT)=0.22, U_1/k_B=73 K and U_2/k_B=235 K. The different interaction potential of the loose spins with ferromagnetic layers 1 and 2, i.e. $U_1 \neq U_2$, is characteristic for the loose spins being predominantly interfacial.

Whereas the analysis of the present results within the loose spin model requires $U_1 \neq U_2$, Strijkers and coworkers were able to analyze the biquadratic coupling in Fe/Si/Fe trilayers assuming U_1=U_2[6], which means that the loose spin entities are randomly distributed throughout the spacer layer. This behavior is probably related to the diffusive nature of Fe/Si and Si/Fe interfaces, resulting in the formation of different silicides[7] and the presence of loose spin entities throughout the whole spacer. Co-evaporated spacer layers grown with a low deposition rate at 150°C, on the other hand, are more homogenous. This results in the dominating presence of interfacial loose spins, characterized by significantly different interaction potentials, U_1 and U_2, with both ferromagnetic layers.

The effective bilinear coupling J_1, deduced from the magnetization measurements, is the sum of: (i) the intrinsic bilinear coupling J_1^{int} across iron monosilicide, i.e., without scattering on loose spins, and (ii) the indirect bilinear coupling J_1^{ls} mediated by the loose spins[13]. Therefore, we fit the temperature dependence of the bilinear coupling J_1 to the expression

$$J_1(T) = J_1^{int}(T) + r \times J_1^{ls}(T). \quad (3)$$

The set of loose spin interaction parameters, obtained from fitting the temperature dependence of the biquadratic coupling, is used to calculate $J_1^{ls}(T)$ with the model of Slonczewski[13]. The parameter r accounts for a possible reduction of the bilinear loose spin contribution $J_1^{ls}(T)$. Such a reduction is attributed to an averaging out process caused by a distribution of interaction strengths between loose spins and the magnetic layers[18]. The resulting fit for $J_1(T)$ is shown as the solid line through the data points in figure 4(e). The dashed line and the solid line in figure 4(f) represent the intrinsic bilinear coupling $J_1^{int}(T)$ and the reduced bilinear loose spin contribution $r \times J_1^{ls}(T)$, respectively. A significant reduction of the bilinear loose spin contribution, r=0.41, is found.

We find a linear temperature dependence for J_1^{int}. A similar temperature dependence has been reported in Fe/Si/Fe sandwiches for the driving intrinsic bilinear coupling[6]. But, unlike the present results where a substantial bilinear loose spin contribution is identified, Strijkers *et al.* found only a negligible bilinear loose spin contribution. As stated in the previous paragraph, this is attributed to an averaging out process caused by the distribution of interaction strengths between the loose spins and the magnetic layers[18]. Such a distribution is much less pronounced for homogenous, co-evaporated spacer layers, where presumably only interfacial loose spins are present. Therefore, a much smaller reduction of the bilinear loose spin contribution is expected in Fe/FeSi/Fe trilayers as compared to Fe/Si/Fe sandwiches.

V. THICKNESS DEPENDENCE OF THE INTERLAYER COUPLING

The fits to the loose spin based model introduced in the previous section converged systematically towards c(RT)≈20% and U_2/k_B ≈235 K for various spacer thicknesses. U_1/k_B, on the other hand, decreases with increasing silicide thickness. Figure 5 displays the room temperature spacer thickness dependence of the different coupling terms. The spacer thickness region exhibiting antiferromagnetic coupling is limited at the thinner side by the increasingly dominant ferromagnetic coupling due to inhomogeneities, pinholes or discontinuities of the spacer layer. For $t_{FeSi} \geq 20$ Å, the coupling terms become very small, while for the intermediate spacer thicknesses, 10 Å $\leq t_{FeSi} \leq$ 20 Å, the coupling coefficients exhibit an exponential spacer thickness dependence:

$$J \sim \exp(-t_{FeSi}/\lambda). \quad (4)$$

This observation establishes the existence of an exponential thickness dependence of antiferromagnetic coup-

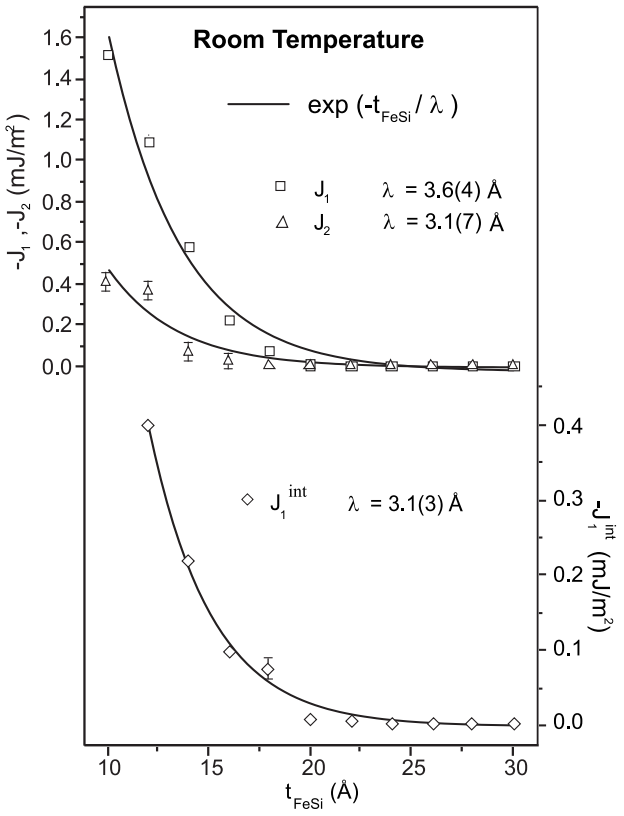

FIG. 5: The different coupling coefficients at room temperature versus spacer thickness t_{FeSi} as derived from magnetization measurements on Fe(80 Å)/^{57}Fe$_{0.50}$Si$_{0.50}$/Fe(40 Å) sandwiches. The solid lines are exponential fits to the data using eq. (4).

ling across epitaxial, semi-metallic iron monosilicide spacer layers. The decay length λ lies between 3 Å and 4 Å for all coupling coefficients and indicates that they are intimately related as implicitly assumed in the loose spin model[13]. At low temperature a similar behavior is found.

VI. DISCUSSION

We interpreted the biquadratic contribution to the interlayer coupling within the framework of the loose spin model. Alternative mechanisms that can account for the magnitude of J_2 in figure 4(c) are the thickness[14] or the composition[19,20] fluctuation models. According to both mechanisms, J_2 arises from magnetic frustration that is caused by lateral variations in the type of the interlayer coupling. For monosilicide interlayers the bilinear coupling J_1 always favors an antiparallel alignment ($J_1 < 0$) of the moments in both magnetic layers[21], and therefore, lateral thickness variations cannot lead to a frustration effect. Hence, an interpretation of biquadratic coupling in terms of the thickness fluctuation model is not appropriate. On the other hand, biquadratic coupling that is caused by the presence of composition fluctuations[19,20] cannot be excluded. However, we believe that this model, in contrast to the loose spin model, has difficulties to explain the similar, non-monotonous temperature dependence of the bilinear and the biquadratic coupling that is shown in panels 4(c) and 4(e) for our samples with prevailing bilinear coupling.

Our measurements revealed an exponential thickness dependence of the coupling coefficients in Fe/CsCl-Fe$_{0.50}$Si$_{0.50}$/Fe. An exponential thickness dependence was observed in Fe/Si/Fe trilayers[6,22,23], where it is attributed to either the specific electronic properties of the monosilicide phase[6,22] or to the quantum interference model for nonconducting spacers[6,22,23].

The quantum interference model[24] predicts an exponential decay of the antiferromagnetic coupling strength for nonconducting spacers but oscillatory coupling for conductive spacers. This interpretation is not appropriate for the present Fe/CsCl-Fe$_{0.50}$Si$_{0.50}$ system, because resistance measurements show a conductive nature of the monosilicide phase, while the antiferromagnetic coupling strength decays exponentially. The model describing how an amorphous conductive spacer leads to an exponential thickness dependence of RKKY-type interlayer coupling[25] is not suitable either, because CEMS, RHEED and XRD experiments reveal the presence of a well-defined crystalline monosilicide with the CsCl phase for all our samples[15].

We relate the exponential thickness dependence of the antiferromagnetic coupling across epitaxial iron monosilicide spacer layers with the CsCl structure to the semimetallic nature of this metastable phase. An exponential coupling behavior is reported by Shi *et al.*[26] for spacer materials that exhibit a pronounced peak in the electronic density of states (DOS) just above the Fermi level together with a very low DOS at the Fermi level. Recently, several groups found that iron monosilicide in the metastable CsCl-phase displays such a strong peak in the electronic density of states, in addition to a reduced (but non-zero) density of states at the Fermi level[21,27,28]. This is in qualitative agreement with our transport measurements and explains the observed exponential thickness dependence of the coupling coefficients. *Ab initio* calculations performed on Fe/CsCl-Fe$_{0.50}$Si$_{0.50}$ by Pruneda *et al.*[21] further corroborate the presence of an exponential thickness dependence of the interlayer coupling across metastable iron monosilicide.

VII. CONCLUSIONS

We have studied the interlayer exchange coupling in well-defined MBE-grown Fe/CsCl-Fe$_{0.50}$Si$_{0.50}$/Fe trilayers. Both strong bilinear and biquadratic coupling coefficients are obtained, exhibiting a non-monotonous temperature dependence. This behavior is explained within the framework of Slonczewski's loose spin model,

assuming a temperature dependent concentration of paramagnetic entities. A substantial loose spin contribution to the bilinear coupling strength is found. In spite of the conductive nature of the monosilicide spacer and its excellent crystallinity no evidence of oscillatory exchange coupling with increasing monosilicide thickness is found. Instead, an exponential thickness dependence with a large decay length is obtained. This behavior is characteristic for a new type of exchange coupling across semi-metallic spacers, in agreement with *ab initio* calculations[21] and coupling theories[26].

Acknowledgments

This work was supported by the F.W.O.-Vlaanderen projects G.0498.04 and G.0194.00, IUAP P5/1 and GOA(KULeuven). It was co-financed by the European Commission in the frame of FP6 via STREP No. NMP4-CT-2003-001516 (DYNASYNC). J. Meersschaut and C. L'abbé thank the Belgian Science Foundation (F.W.O.-Vlaanderen) for financial support.

* E-mail: johan.meersschaut@fys.kuleuven.ac.be

[1] S. Toscano, B. Briner, H. Hopster, and M. Landolt, J. Magn. Magn. Mater. **114**, L6 (1992).
[2] E. E. Fullerton, J. E. Mattson, S. R. Lee, C. H. Sowers, Y. Y. Huang, G. Felcher, and S. D. Bader, J. Magn. Magn. Mater. **117**, L301 (1992).
[3] A. Chaiken, R. P. Michel, and M. A. Wall, Phys. Rev. B **53**, 5518 (1996).
[4] J. E. Mattson, S. Kumar, E. E. Fullerton, S. R. Lee, C. H. Sowers, M. Grimsditch, S. D. Bader, and F. T. Parker, Phys. Rev. Lett. **71**, 185 (1993).
[5] M. Hansen, *Constitution of Binary Alloys* (McGraw-Hill book Company, 1958).
[6] G. J. Strijkers, J. T. Kohlhepp, H. J. M. Swagten, and W. J. M. de Jonge, Phys. Rev. Lett. **84**, 1812 (2000).
[7] G. J. Strijkers, J. T. Kohlhepp, H. J. M. Swagten, and W. J. M. de Jonge, Phys. Rev. B **60**, 9583 (1999).
[8] R. R. Gareev, D. E. Bürgler, M. Buchmeier, D. Olligs, R. Schreiber, and P. Grünberg, Phys. Rev. Lett. **87**, 157202 (2001).
[9] Y. Endo, O. Kitakami, and Y. Shimada, Phys. Rev. B **59**, 4279 (1999).
[10] E. E. Fullerton and S. D. Bader, Phys. Rev. B **53**, 5112 (1996).
[11] J. T. Kohlhepp and F. J. A. den Broeder, J. Magn. Magn. Mater. **156**, 261 (1996).
[12] J. Kohlhepp, M. Valkier, A. van der Graaf, and F. J. A. den Broeder, Phys. Rev. B **55**, R696 (1997).
[13] J. Slonczewski, J. Appl. Phys. **73**, 5957 (1993).
[14] J.C. Slonczewski, Phys. Rev. Lett. **67**, 3172 (1991).
[15] B. Croonenborghs, F. M. Almeida, S. Cottenier, M. Rots, A. Vantomme, and J. Meersschaut, Appl. Phys. Lett. **85**, 200 (2004).
[16] R. R. Gareev, L. L. Pohlmann, S. Stein, D. E. Bürgler, P. Grünberg, and M. Siegel, J. Appl. Phys. **93**, 8038 (2003).
[17] J. Meersschaut, C. L'abbé, M. Rots, and S. D. Bader, Phys. Rev. Lett. **87**, 107201 (2001).
[18] G. J. Strijkers, J. T. Kohlhepp, H. J. M. Swagten, and W. J. M. de Jonge, J. Appl. Phys. **87**, 5452 (2000).
[19] J.F. Bobo, H. Kikuchi, O. Redon, E. Snoeck, M. Piecuch, and R.L. White, Phys. Rev. B **60**, 4131 (1999).
[20] D.B. Fulghum and R.E. Camley, Phys. Rev. B **52**, 13436 (1995).
[21] J. M. Pruneda, R. Robles, S. Bouarab, J. Ferrer, and A. Vega, Phys. Rev. B **65**, 024440 (2001).
[22] J. J. de Vries, J. Kohlhepp, F. J. A. den Broeder, R. Coehoorn, R. Jungblut, A. Reinders, and W. J. M. de Jonge, Phys. Rev. Lett. **78**, 3023 (1997).
[23] R. R. Gareev, D. E. Bürgler, M. Buchmeier, R. Schreiber, and P. Grünberg, J. Magn. Magn. Mater. **240**, 235 (2002).
[24] P. Bruno, Phys. Rev. B **52**, 411 (1995).
[25] D. E. Bürgler, D. M. Schaller, C. M. Schmidt, F. Meisinger, J. Kroha, J. McCord, A. Hubert, and H. J. Güntherodt, Phys. Rev. Lett. **80**, 4983 (1998).
[26] Z. P. Shi, M. Levy, and J. L. Fry, Europhys. Lett. **26**, 473 (1994).
[27] E. G. Moroni, W. Wolf, J. Hafner, and R. Podloucky, Phys. Rev. B **59**, 12860 (1999).
[28] M. Fanciulli, G. Weyer, A. Svane, N. E. Christensen, H. von Känel, E. Müller, N. Onda, L. Miglio, F. Tavazza, and M. Celino, Phys. Rev. B **59**, 3675 (1999).